A potential well model for host-guest chemistry in double-network hydrogels toward mechanochemical coupling and toughening

Ziyu Xing[1], Haibao Lu[1,4], Denvid Lau[2,4] and Yong-Qing Fu[3,4]

[1]National Key Laboratory of Science and Technology on Advanced Composites in Special Environments, Harbin Institute of Technology, Harbin 150080, China

[2]Department of Architecture and Civil Engineering, City University of Hong Kong, Tat Chee Avenue, Kowloon, Hong Kong

[3]Faculty of Engineering and Environment, University of Northumbria, Newcastle upon Tyne, NE1 8ST, UK

[4]E-mail: luhb@hit.edu.cn; denvid.lau@cityu.edu.hk; richard.fu@northumbria.ac.uk

Abstract: Different from the conventional single-network hydrogels, double-network (DN) hydrogels have attracted great research interest due to their ultra-high toughness, however, their working principles behind complex mechanochemical coupling have not been fully understood. In this study, an extended potential well model is formulated to investigate host-guest chemistry and free-energy trap effect, coupled in the DN hydrogels undergoing mechanochemical toughening. According to the Morse potential and mean field model, the newly established potential well model can describe the coupled binding of host brittle network and guest ductile network in the DN hydrogels. A free-energy equation is further proposed to describe working principles of mechanochemical coupling and toughening mechanisms using the depth, width and trap number of potential wells, which determine the barrier energy of host brittle network, mesh size of guest ductile network and mechanochemical host-guest

interactions of these two networks, respectively. Finally, effectiveness of the proposed model is verified using finite-element analysis and experimental results of various DN hydrogels reported in literature. This study clarifies the linking of mechanochemical coupling and toughening mechanisms in DN hydrogels having the host-guest chemistry from both brittle and ductile networks using the potential well model.

Keywords: hydrogel; potential well; host-guest chemistry; mechanochemical

1. Introduction

Hydrogel recently becomes one of the most popular soft matters [1-5], and is highly absorbent yet can maintain its well-defined biocompatibility and high stretchability for various applications, especially in artificial muscle [6], artificial cartilage [7], wound dressing [8], strain sensor [9] and bioelectronics [10-12]. However, mechanical toughness of the conventional hydrogels is remarkably low [11,12], which seriously limits their practical and potential applications.

Previous studies [11-17] reported that the single hydrogel network has problems to achieve a high deformability and low toughness, therefore, double network (DN) hydrogels have been proposed and currently attracted wide attentions. In the DN hydrogels, there are two types of network structures, i.e., brittle network and ductile network, which are able to resist external loads and improve mechanical properties by sacrifice of covalent bonds and elastic stretchability, respectively [11-17]. There have been numerous studies to understand the mechanochemical coupling and achieve ultra-high toughness and strength of DN hydrogels using methodologies such as continuum mechanics [18-20], mechanochemistry [21-24], multiple networks [25,26],

and phase separation [27,28]. However, working principles behind the mechanochemical toughening of DN hydrogels have not been fully understood, even though great efforts have been made.

In this study, an extended potential well model is formulated to describe the host-guest chemistry based on free-energy trapping effects reported in DN hydrogels, using the Morse potential [29-31] and mean field models [32,33]. A constitutive relationship between the potential wells and molecular network structures of DN hydrogels has been developed using free-energy equations. Depth, width and trap number of potential wells have been applied to characterize the barrier energy of host brittle network, mesh size of guest ductile network, and host-guest interaction of these two networks, respectively, based on the rubber elasticity theory [34]. Finally, effectiveness of the proposed model has been verified using finite-element analysis (FEA) and various experimental results of DN hydrogels reported in literature [6,22-25].

2. Theoretical framework

As illustrated in Figure 1, the DN hydrogel is synthesized based on the methodology of host-guest chemistry, where the guest ductile networks are trapped inside the host brittle networks. Thermodynamic and mechanical behaviors of guest ductile networks are critically determined by the host brittle networks, which undergo mechanochemical coupling, causing the decreased barrier energies and changes of thermodynamic behaviors of guest ductile networks. Therefore, the potential well model [30,32] has been employed to describe the host-guest interactions and

free-energy trap effect in the DN hydrogels, where the width and depth of the potential wells are used to describe barrier energies (F_{ba}) of the host brittle networks and mesh sizes (ξ) of the guest ductile networks, respectively. Furthermore, the trap number (N_{el}) of potential wells is introduced to characterize the host-guest interactions between the host brittle network and guest ductile network, undergoing the mechanochemical coupling.

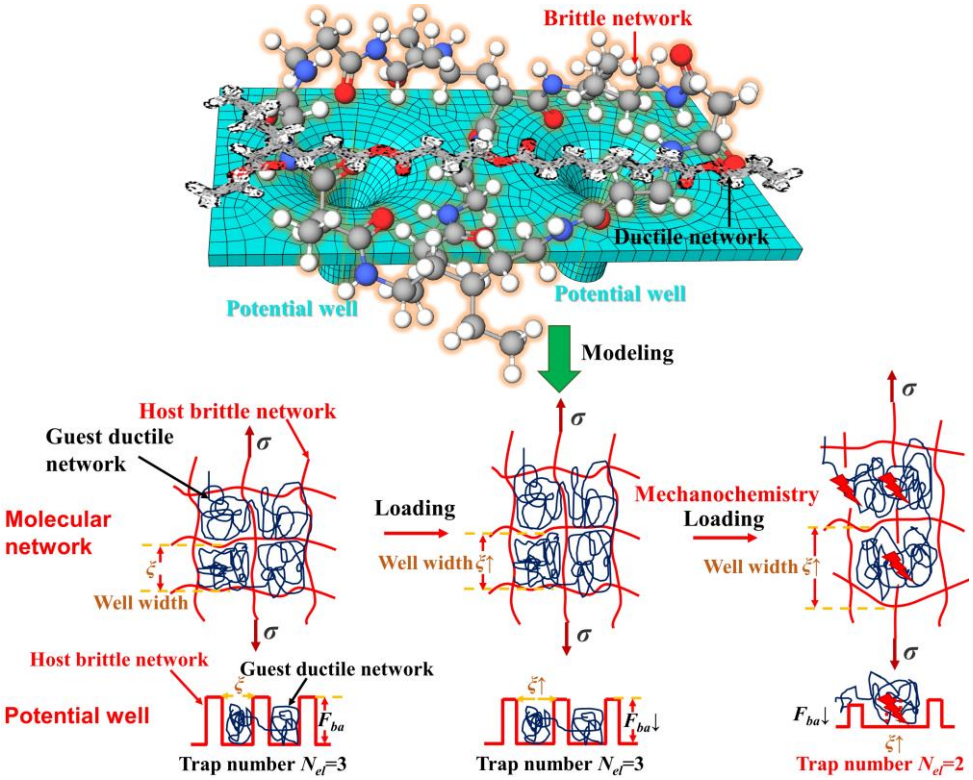

Figure 1. Schematic illustrations of potential well model for the host-guest chemistry and free-energy trap effect in DN hydrogel, where the well depth and width are used to describe the barrier energy (F_{ba}) of host brittle network and mesh size (ξ) of the guest ductile network.

According to the Flory's mean field model [32,33], there are three types of free energies for host-guest interactions in the DN hydrogels, i.e., tail free energy (F_{tail}), tie free energy (F_{tie}) and barrier energy (F_{ba}), which are determined by the parameters of confinement entropy [32,33], excluded volume [35], and electrostatic interactions

[36,37], respectively,

$$\frac{F_{tail}}{k_BT}=\ln(\frac{\xi}{4b})+\frac{2\pi^2}{3}(\frac{b}{\xi})^2m+\frac{3v}{\pi}(\frac{b}{\xi})^3m^2-\frac{\rho_c l_B}{e^{\kappa b}}\frac{b}{\xi} \tag{1}$$

$$\frac{F_{tie}}{k_BT}=\ln(\frac{\xi^5}{16\pi b^5})+\frac{2\pi^2}{3}(\frac{b}{\xi})^2m+\frac{3v}{\pi}(\frac{b}{\xi})^3m^2-\frac{\rho_c l_B}{e^{\kappa b}}\frac{b}{\xi} \tag{2}$$

$$\frac{F_{ba}}{k_BT}=\ln(\frac{\xi^8}{96b^8})-\frac{\rho_c l_B}{e^{\kappa b}}\frac{b}{\xi} \tag{3}$$

where k_B=1.38×10^{-23} J/K is the Boltzmann constant, T is the ambient temperature, ρ_c is the linear charge density, m is the number of chains of ductile network in the potential well, b is length of chain of the ductile network, v=1 is the excluded volume, l_B is the Bjerrum length [32], and κ is the inverse Debye length [32].

According to the lattice model [38] and Flory theory [39], the mesh sizes (ξ) of guest ductile networks and barrier energies (F_{ba}) of host brittle networks are used to describe width and depth of potential wells using the potential well model [32]. Due to the mechanochemical coupling, the change in the free energy (ΔF_t) of the potential well can be expressed as [32],

$$\begin{aligned}&\frac{\Delta F_t}{k_BT}=\frac{F_{tail}(\xi,m)}{k_BT}+\frac{F_{tie}(\xi,m)}{k_BT}-\frac{F_{tail}(\sqrt{2}\xi,2m)}{k_BT}=\\&\ln(\frac{\xi^5}{16\sqrt{2}\pi b^5})+\frac{2\pi^2}{3}(\frac{b}{\xi})^2m+(2-\sqrt{2})\frac{3v}{\pi}(\frac{b}{\xi})^3m^2+(\sqrt{2}-2)\frac{\rho_c\xi l_B}{be^{\kappa b}}\end{aligned} \tag{4a}$$

$$\begin{aligned}&2\frac{F_{tie}(\xi,m)}{k_BT}-\frac{F_{tie}(\sqrt{2}\xi,2m)}{k_BT}=\\&\ln(\frac{\xi^5}{64\sqrt{2}\pi b^5})+\frac{2\pi^2}{3}(\frac{b}{\xi})^2m+(2-\sqrt{2})\frac{3v}{\pi}(\frac{b}{\xi})^3m^2+(\sqrt{2}-2)\frac{\rho_c\xi l_B}{be^{\kappa b}}\\&=\frac{\Delta F_t}{k_BT}-\ln(4)\end{aligned} \tag{4b}$$

Based on the equation (4a), the change in free energy (ΔF) of DN hydrogels is

obtained as,

$$\begin{aligned}\Delta F &= N_{cm}(F_{ba}+\Delta F_t)\\ &= N_{cm}k_BT[\frac{2\pi^2}{3}(\frac{b}{\xi})^2 m+(2-\sqrt{2})\frac{3\nu}{\pi}(\frac{b}{\xi})^3 m^2+(\sqrt{2}-1)\frac{\rho_c l_B}{e^{\kappa b}}\frac{b}{\xi}+13\ln(\frac{\xi}{b})]\end{aligned} \quad (5)$$

where N_{cm} is the molar number of potential wells involved into the mechanochemical reactions for brittle network.

Based on the Morse potential (F_M) [29] and bread-spring model [29-31], a constitutive relationship of applied force (f) and stretching strain (ΔR) can be introduced for the covalent bonds in the brittle network undergoing mechanochemical coupling, i.e.,

$$F_M = D_e(1-e^{-\alpha\Delta R})^2 - f\Delta R \quad (6)$$

$$\Delta R = \frac{1}{\alpha}\log\frac{2}{1-\sqrt{1-2f/\alpha D_e}} \quad (7)$$

where D_e=501.6 kJ/mol is the maximum potential energy of the covalent bond [29], α=0.5 Å^{-1} is the inverse length scale for reaching this maximum stretching ratio [29].

Combining equations (6) and (7), the Morse potential (F_M) as a function of stretching strain (ΔR) of the covalent bond can be written using the following equation [29],

$$F_M = D_e(1-e^{-\alpha\Delta R})^2 - 2\alpha\Delta R D_e e^{-\alpha\Delta R}(1-e^{-\alpha\Delta R}) \quad (8)$$

According to the rubber elasticity theory [34], the stretching strain (ΔR) of covalent bonds can be rewritten as,

$$\Delta R = \Delta R_0(\lambda - \frac{1}{\lambda^2}) \quad (9)$$

where ΔR_0 is the affine motion coefficient, and λ is the elongation ratio [34].

Based on the statistical mechanics, the number of covalent bonds (N_{cm}) can be scaled up using the mechanochemical probability (p) of the covalent bonds in the brittle network [29,35],

$$p \propto (\tau^{-1})^{-2} \propto \tau^2 \propto \exp(-\frac{2F_M}{k_B T}) \tag{10}$$

$$N_{cm} = pN_{el} = N_{el} p_0 \exp[-2D_e \frac{(1-e^{-\alpha\Delta R}) - 2\alpha\Delta R e^{-\alpha\Delta R}}{k_B T / (1-e^{-\alpha\Delta R})}] \tag{11}$$

$$\Delta F_{cm} = N_{cm} F_{ba} = N_{el} F_{ba} p_0 \exp[-2D_e \frac{(1-e^{-\alpha\Delta R}) - 2\alpha\Delta R e^{-\alpha\Delta R}}{k_B T / (1-e^{-\alpha\Delta R})}] \tag{12}$$

where τ is the mean breaking time of covalent bonds, p_0 is the normalized initial mechanochemical probability, N_{el} is the total number of potential wells undergoing the elastic stretching, and ΔF_{cm} is the mechanochemical free energy.

Furthermore, the mesh size (ξ), which is used to characterize the width of potential wells, is governed by the Cauchy-Green tensor (I_1) and can be described by the elongation ratios (i.e., λ_1, λ_2 and λ_3, or the elongation ratios along three directions, respectively) [18-20],

$$\xi = \xi_0 \sqrt{\frac{I_1}{3}} \tag{13a}$$

$$I_1 = \lambda_1^2 + \lambda_2^2 + \lambda_3^2 \tag{13b}$$

where ξ_0 is the initial mesh size of brittle network, and I_1 is the strain invariant.

The stress (σ) as a function of elongation ratio (λ) for the DN hydrogel undergoing the uniaxial tensile stretching can be obtained,

$$\sigma = \frac{d\Delta F}{d\lambda} = N_{cm} k_B T [\frac{(\sqrt{2}-1)\rho_{ea}\xi_0}{2\sqrt{3}b\sqrt{I_1}} + \frac{13}{2I_1} - \frac{2m\pi^2 b^2}{\xi_0^2 I_1^2} - \frac{27\sqrt{3}\nu m^2 b^3}{(2+\sqrt{2})\pi\xi_0^3 I_1^{5/2}}] I_1' \tag{14a}$$

$$I_1 = \lambda^2 + 2/\lambda \tag{14b}$$

where $\rho_{ea}=\frac{\rho_c l_B}{e^{\kappa b}}$ is the electrostatic attraction parameter. Assuming volume invariance of an isotropic material, i.e., $\lambda_1\lambda_2\lambda_3=1$ [34], the relationships of $\lambda_1=\lambda$ and $\lambda_2=\lambda_3=\lambda^{-1/2}$ can be obtained, and then used for the DN hydrogels under the uniaxial tensile stretching.

Substituting equation (11) into (14a), the constitutive relationship of stress (σ) as a function of elongation ratio (λ) for the DN hydrogel can be finally obtained,

$$\sigma = N_{el}k_BT\underbrace{p_0\exp[-2D_e\frac{(1-e_R)-\alpha\Delta R_0 I' e_R}{k_BT/(1-e_R)}]}_{\text{Mechanochemistry}} \times\underbrace{[\frac{(\sqrt{2}-1)\rho_{ea}\xi_0}{2\sqrt{3}b\sqrt{I_1}}+\frac{13}{2I_1}-\frac{2m\pi^2b^2}{\xi_0^2I_1^2}-\frac{27\sqrt{3}vm^2b^3}{(2+\sqrt{2})\pi\xi_0^3I_1^{5/2}}]I_1'}_{\text{Elasticity and yielding}} \tag{15a}$$

$$I_1=\lambda^2+2/\lambda \tag{15b}$$

$$e_R=\exp[-\alpha\Delta R_0(\lambda-1/\lambda^2)] \tag{15c}$$

where $I_1^{'}=2\lambda-2/\lambda^2$ is the inverse of I_1, e_R is the abbreviation of affine motion, and $\varepsilon=\lambda-1$ is the engineering strain [6,22-25].

To verify the applicability of equation (15), effects of affine motion coefficients of covalent bonds (ΔR_0) and mesh size (ξ_0) of brittle networks on the mechanical behaviors of DN hydrogels have been studied using equation (15). The obtained results are plotted in Figure 2. Parameters used in the calculations are $N_{el}k_BTp_0$=0.1 MPa, $2D_e/k_BT$=405, b=1 nm, ξ_0=10 nm, ΔR_0=0.016 Å, m=40 and ρ_{ea}=0.6. Results show that the stress is gradually increased from 0.54 MPa, 0.83 MPa, 1.34 MPa, 2.27 MPa to 4.01 MPa at the same elongation ratio of λ=1000% and the mesh size of ξ_0=10 nm, with the affine motion coefficient of covalent bond (ΔR_0) increased from 0.012 Å,

0.014 Å, 0.016 Å, 0.018 Å to 0.020 Å, as plotted in Figure 2(a). The effect of mesh size (ξ_0) of brittle network on stress-strain behavior is further studied using equation (15). The obtained results are plotted in Figure 2(b). The analytical results reveal that with an increase in the mesh size (ξ_0) of brittle network from 7.5 nm, 10 nm, 12.5 nm, 15 nm to 17.5 nm, the stress is increased from 0.58 MPa, 0.61 MPa, 0.63 MPa, 0.65 MPa to 0.67 MPa, at the same elongation ratio of λ=700% and affine motion coefficient of ΔR_0=0.016 Å. Clearly, an increase in the width of potential wells (ξ_0) enhances the strength of DN hydrogels, at the same barrier energy (F_{ba}) and the same total number of potential wells (N_{el}).

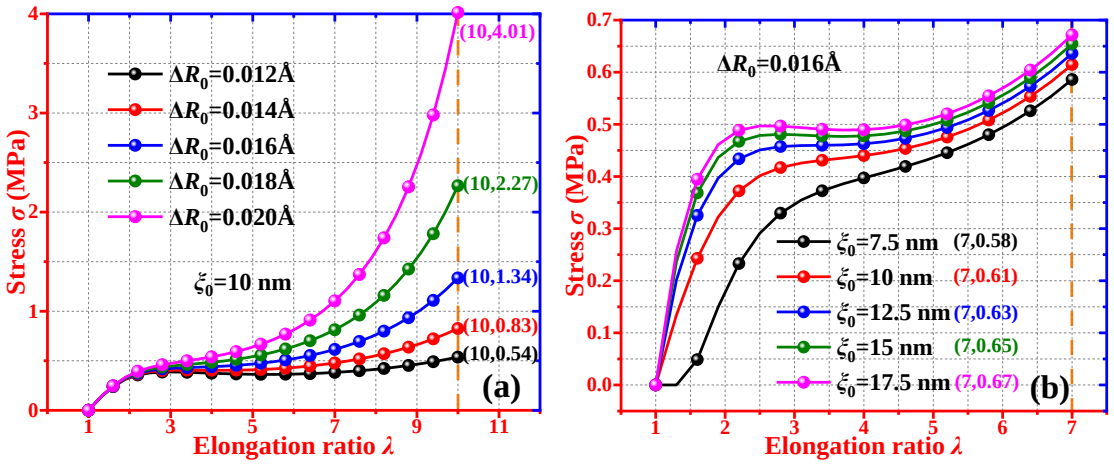

Figure 2. Analytical results of equation (15) for the effect of mechanochemical coupling on the stress-elongation ratio behavior of DN hydrogel. (a) Effect of affine motion coefficient of covalent bond (ΔR_0), at a given constant of mesh size ξ_0 =10 nm. (b) Effect of mesh size (ξ_0) of brittle network, at a given constant of affine motion coefficient of covalent bond ΔR_0=0.016 Å.

To further verify the effectiveness of equation (15), analytical results of stresses for DN hydrogels of PNaAMPS/PAAm (PNaAMPS: poly(2-acrylamido-2-methylpropanesulfonic acid) sodium salt; PAAm: poly(acrylamide)) as a function of strain were obtained. The results are plotted in

Figure 3(a), together with their experimentally obtained data reported in Ref. [6]. The parameters used in equation (15) for calculations are $N_{el}k_BTp_0$=0.133 MPa, $2D_e/k_BT$=405 [29], ΔR_0=0.0152 Å, ξ_0/b=10, m=44 and ρ_{ea}=0.6. It is revealed that these analytical results of the PNaAMPS/PAAm DN hydrogels agree well with the experimental data, with errors of ±1.43%. During deformation, the hydrogel undergoes three-stage mechanical behaviors, i.e., elasticity, yielding and mechanochemistry, in the strain (ε) ranges from 0~50%, 50%~200% and 200%~750%, respectively. Furthermore, the strong mechanochemical coupling effect in the DN hydrogel results in an ultra-high stress at the same strain.

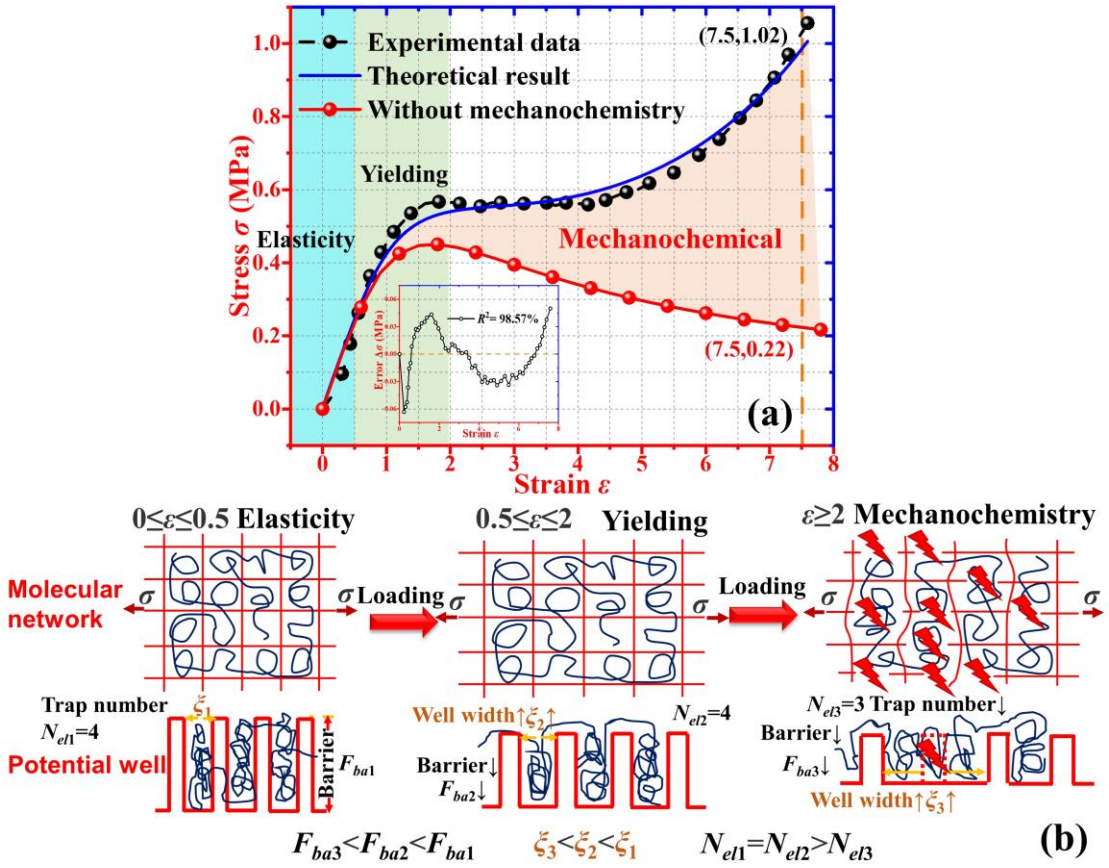

Figure 3. Analytical results and experimental data [6] of stress-strain curve of PNaAMPS/PAAm DN hydrogel. (b) Schematic illustrations of molecular networks undergoing elastic, yielding and mechanochemical behavior using potential well in response to external stress.

Figure 3(b) illustrates the working principle of potential wells for the host-guest chemistry and mechanical behaviors of DN hydrogel. The width (mesh size, ξ) of potential wells determines the elasticity of host brittle network and DN hydrogels. Whereas the depth (barrier energy, F_{ba}) of potential wells determines the yielding behavior of DN hydrogels caused by the host-guest interactions between the host brittle network and guest ductile network. Finally, the mechanochemical behavior of DN hydrogel is determined by the trap number (N_{el}) of potential wells. Increase of this trap number results in an increase in the mechanochemical probability (p) of the host brittle network, thus causing decreased the barrier energy (F_{ba}).

3. Finite-element analysis (FEA) and experimental verification

3.1 FEA simulation

To further investigate effects of width (mesh size, ξ), depth (barrier energy, F_{ba}) and trap number (N_{el}) of potential wells, we used FEA simulations to study the constitutive stress-strain relationship in the DN hydrogels by considering all the above three factors. The FEA models are shown in Figure 4. The brittle networks were designed as a sparse regular network (20 mm × 20 mm). In the simulations, the Young's modulus and Poisson's ratio of brittle networks were chosen as 1 MPa and 0.45, respectively. An 8-node hexahedron element, C3D8R, was used to perform the calculations, and 5000 elements were used to model the whole unit. The spatial properties of the main network (i.e., the host brittle network in this study) is determined by the width (ξ) and trap number (N_{el}) of potential wells, which can be written as $\xi^{-2} \propto N_{el}$. Here the variable of ξ^{-2} has been employed to represent the

attributes of widths (ξ) and trap numbers (N_{el}) of potential wells to the space structure of the main network.

There are three types of potential wells for the brittle networks, i.e., ξ=5 mm, F_{ba}=2 mm and N_{el}=3; ξ=5 mm, F_{ba}=4 mm and N_{el}=2; ξ=12 mm, F_{ba}=4 mm and N_{el}=3. In the uniaxial stretching, the decrease of depth (barrier energy, F_{ba}) of potential wells from 4 mm to 2 mm has decreased the stress from 0.52 MPa to 0.45 MPa. The decrease in trap number (N_{el}) from 3 to 2 has decreased the stress from 0.52 MPa to 0.47 MPa. Whereas the increase of the width (mesh size, ξ) from 5 mm to 12 mm has increased the stress from 0.52 MPa to 0.56 MPa. These FEA simulation results prove our hypothesis that the mechanical behaviors of DN hydrogels are determined by the width (ξ), depth (F_{ba}) and trap number (N_{el}) of potential wells.

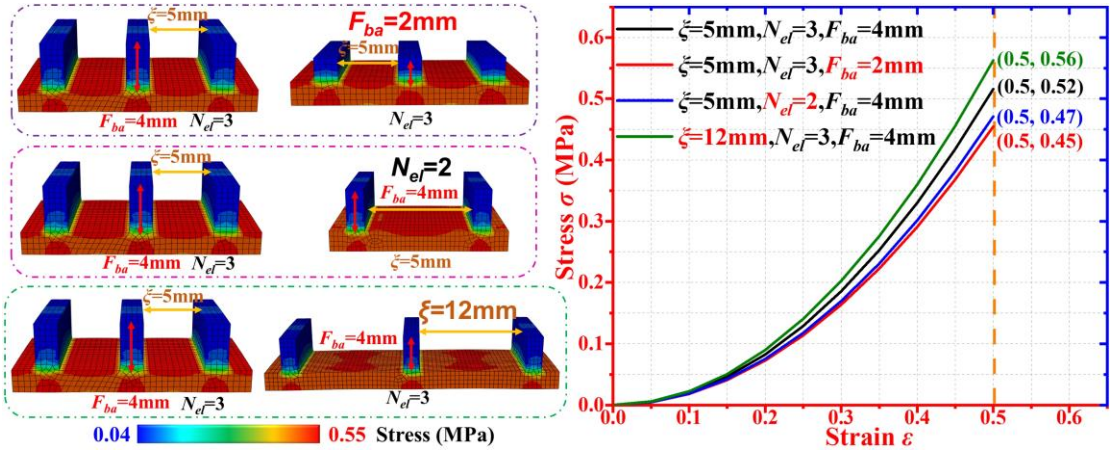

Figure 4. FEA simulations of the effects of width (mesh size, ξ), depth (barrier energy, F_{ba}) and trap number (N_{el}) of potential wells on the constitutive stress-strain relationship of DN hydrogel.

3.2 Experimental verification

3.2.1 Effect of potential well width on the mechanochemical coupling

Experimental data [6,22-25] of DN hydrogels were applied to verify the analytical results generated from the proposed model of equations (12) and (15). Here, $N_{el}k_BTp_0$

is the modulus of DN hydrogel based on the rubber elasticity theory [34], N_{el} is the total number of potential wells undergoing elastic stretching, k_B=1.38×10^{-23} J/K is the Boltzmann constant, T≈298.15 K is the temperature, p_0 is normalized initial mechanochemical probability. ΔR_0 is affine motion coefficient of bond stretches according to rubber elastic theory [34], ξ_0 is the initial mesh size of brittle network (width of potential well), b is length of segment, m is the number of segments of guest ductile network in a potential well. ρ_c is the linear charge density, v=1 is the intersegment excluded volume interaction strength, l_B is the Bjerrum length at which inter-charge interaction energy is k_BT, and κ is the inverse Debye length, $\rho_{ea}=\frac{\rho_c l_B}{e^{\kappa b}}$ is electrostatic attraction parameter [32,35-37]. D_e=501.6 kJ/mol is the maximum potential energy of the unstretched Morse potential of carbon bond [29], which has a relationship of $2D_e/k_BT$=405 [29]. α=0.5 Å^{-1} is an inverse length scale for reaching the maximum stretching [29], $\varepsilon=\lambda$-1 is strain. Finally, the Levenberg-Marquardt optimization algorithm was adopted for all the calculations.

Four groups of experimental data [6,22-25] of DN hydrogels were used to verify the analytical results generated using the proposed models, based on equations (12) and (15), with the chosen parameters as following, T=298.15 K, v=1, D_e=501.6 kJ/mol [29], α=0.5 Å^{-1} [29], and $\varepsilon=\lambda$-1 [6,22-25]. The other parameters used in the calculations using equation (12) are listed in Table 1. Figure 5(a) shows the hysteresis energy *vs.* strain curves for the DN hydrogels of P(BCD-co-AMPS)/PMBAA [22] (BCD: bicyclo[6.2.0]decane, AMPS: 2-acrylamido-2-methylpropane sulfonate; MBAA: N,N'-methylenebisacrylamide). Here 4 mol% or 8 mol% cross-linking

density of MBAA has been used as the ductile network, and reactive strand extension (RSE) has also been introduced to enhance the stretchability of brittle P(BCD-co-AMPS) network [22]. The hysteresis energy is found to gradually increase from 0.022 MJ/m^3, 0.053 MJ/m^3 to 0.079 MJ/m^3 at the same strain of ε=1, for the DN4, DN8 and DN8-RSE hydrogels, respectively.

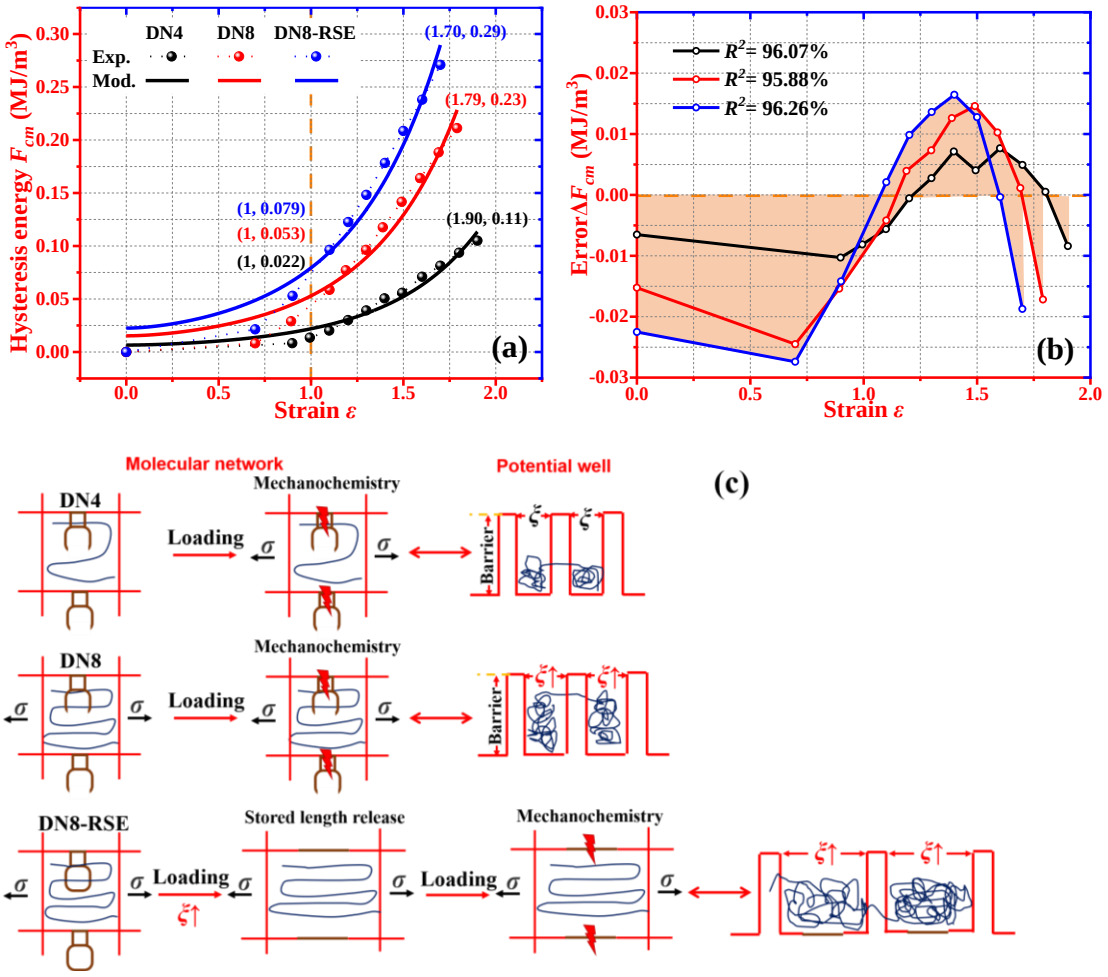

Figure 5. Comparisons of analytical results using equation (12) and experimental data [22] of the hysteresis energy as a function of strain for P(BCD-co-AMPS)/PMBAA DN hydrogels. (a) The hysteresis energy *vs.* strain curves. (b) Divergences of analytical and experimental results of stress. (c) Schematic illustration of the working principle of width (mesh size, ξ) in potential wells.

Figure 5(b) shows the values of correlation index R^2 between the analytical and experimental results, which are 96.07%, 95.88% and 96.26% for the DN4, DN8 and

DN8-RSE hydrogels, respectively. It can be seen that the analytical results obtained using equation (12) agree well with the experimental data ($|\Delta F_{cm}|$<0.03 MJ/m^3). The working mechanism of P(BCD-co-AMPS)/PMBAA DN hydrogels is illustrated in Figure 5(c). With an increase in the molar content of ductile MBAA networks from 4 mol% to 8 mol%, both the well width (mesh size, ξ) and hysteresis energy are increased. Furthermore, the RSE is found to increase well width (mesh size, ξ) of the DN8-RSE hydrogel, thus resulting in an increased hysteresis energy.

Table 1. Values of parameters used in equation (12) for P(BCD-co-AMPS)/PMBAA DN hydrogels.

	$N_{el}F_{ba}p_0$(MJ/m^3)	ΔR_0(Å)	$2D_e/k_BT$
DN4	3.3×10^{-3}	6.63×10^{-2}	405 [29]
DN8	7.6×10^{-3}	6.72×10^{-2}	
DN8-RSE	11.3×10^{-3}	7.66×10^{-3}	

Experimental data [23] of PAMPS/PCDME (PCDME: poly-N-(carboxymethyl)-N, N-di-methyl-2-(methacryloyloxy) ethanaminium) DN hydrogels have further been applied to verify the analytical results generated using the proposed model based on the equation (15). For the PAMPS/PCDME DN hydrogel, the PCDME acts as the ductile network and the PAMPS works as the brittle one [23]. Figure 6(a) plots the constitutive stress-strain relationship of PAMPS/PCDME DN hydrogels with various PCDME molar ratios (R_{mo}) of 10.5 mol/L, 25.6 mol/L and 44.3 mol/L. All the parameters used in the calculations using the equation (15) are listed in Table 2. These analytical and experimental results reveal that the yielding strains are increased from

1.75, 5.73 to 6.53, for the PCDME/PAMPS DN hydrogels with an increase in molar ratio of PCDME (R_{mo}) from 10.5 mol/L, 25.6 mol/L to 44.3 mol/L.

Table 2. Values of parameters used in equation (15) for PAMPS/PCDME DN hydrogels.

R_{mo}(mol/L)	$N_{el}k_BTp_0$(MPa)	ξ_0/b	m	$2D_e/k_BT$	ΔR_0(Å)	ρ_{ea}
10.5	0.302	4	11			
25.6	0.182	7	19	405 [29]	0.016	0.42
44.3	0.087	30	92			

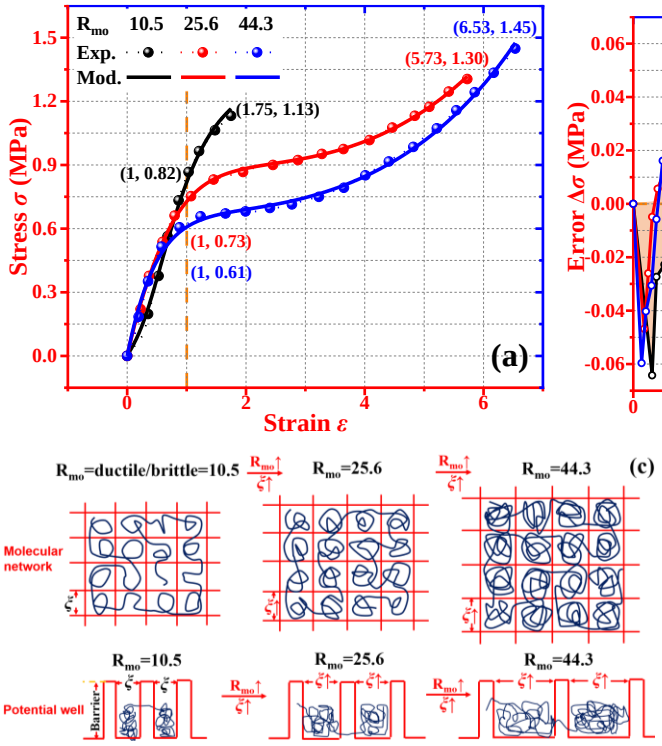

Figure 6. Comparisons of analytical results using equation (15) and experimental data [23] of the stress *vs.* strain for PAMPS/PCDME DN hydrogels, at given various PCDME molar ratios (R_{mo}) of 10.5 mol/L, 25.6 mol/L and 44.3 mol/L. (a) The stress-strain curves. (b) Divergences of analytical and experimental results of stress. (c) Schematic illustration of the effect of width (mesh size, ξ) on the yielding behavior of DN hydrogels with various PCDME molar ratios (R_{mo}).

Figure 6(b) shows the divergences between the analytical and experimental results, obtained by calculating the correlation index (R^2). The obtained R^2 values are 99.37%, 99.87% and 99.70% at molar ratios (R_{mo}) of PCDME of 10.5, 25.6 and 44.3,

respectively. The working principle of ductile PCDME networks in the PAMPS/PCDME DN hydrogels is illustrated in Figure 6(c). With an increase of molar ratio of ductile PCDME network, the increased well width (mesh size, ξ) increases the yielding strain of the DN hydrogel, according to the proposed potential well model based on the equation (15).

3.2.2 Effect of barrier energy on the mechanochemical coupling

Experimental data of PAMPS/PAAm [25] (PAMPS: poly(2-acrylamido-2-methylpropanesulfonic acid) and PVA/PAMPS/PAAm (PVA-DN) (PVA: poly(vinyl alcohol) DN hydrogels were also applied to verify the proposed model based on the equation (15). PVA/PAMPS is applied as the brittle network, whose stiffness (with a modulus of 0.15 MPa) is lower than that of PAMPS brittle network (with a modulus of 0.25 MPa). In this study, 0.1 mol% or 0.6 mol% of 2-oxoglutaric acid has been used as the photoinitiator for crosslinking between two networks [25]. Experimental results revealed that the moduli and stiffness of PAMPS brittle networks were gradually decreased with an increase in the molar content of the photo-initiator. Both the analytical and experimental results are plotted in Figure 7(a). The parameters used in the calculations using equation (15) are listed in Table 3. The stresses are 0.75 MPa, 0.63 MPa, 0.72 MPa and 0.50 MPa for the DN0.1, PVA-DN0.1, DN0.6 and PVA-DN0.6 hydrogels, respectively, at a constant strain of ε=3. Furthermore, results of stress-strain relationship in the DN hydrogels using the classical Mooney-Rivlin (M-R) equation [34] ($\sigma=(2C_1+2C_2/\lambda)(\lambda-1/\lambda^2)$, where C_1 and C_2 are material constants) are plotted, and the analytical results from the proposed

model of equation (15) have good agreements with the experimental results [25]. Figure 7(b) shows the divergences between analytical and experimental results based on the values of correlation coefficient (R^2), which are R^2=98.70%, R^2=94.89%, R^2=99.52% and R^2=94.62% for the DN0.1, PVA-DN0.1, DN0.6 and PVA-DN0.6, respectively.

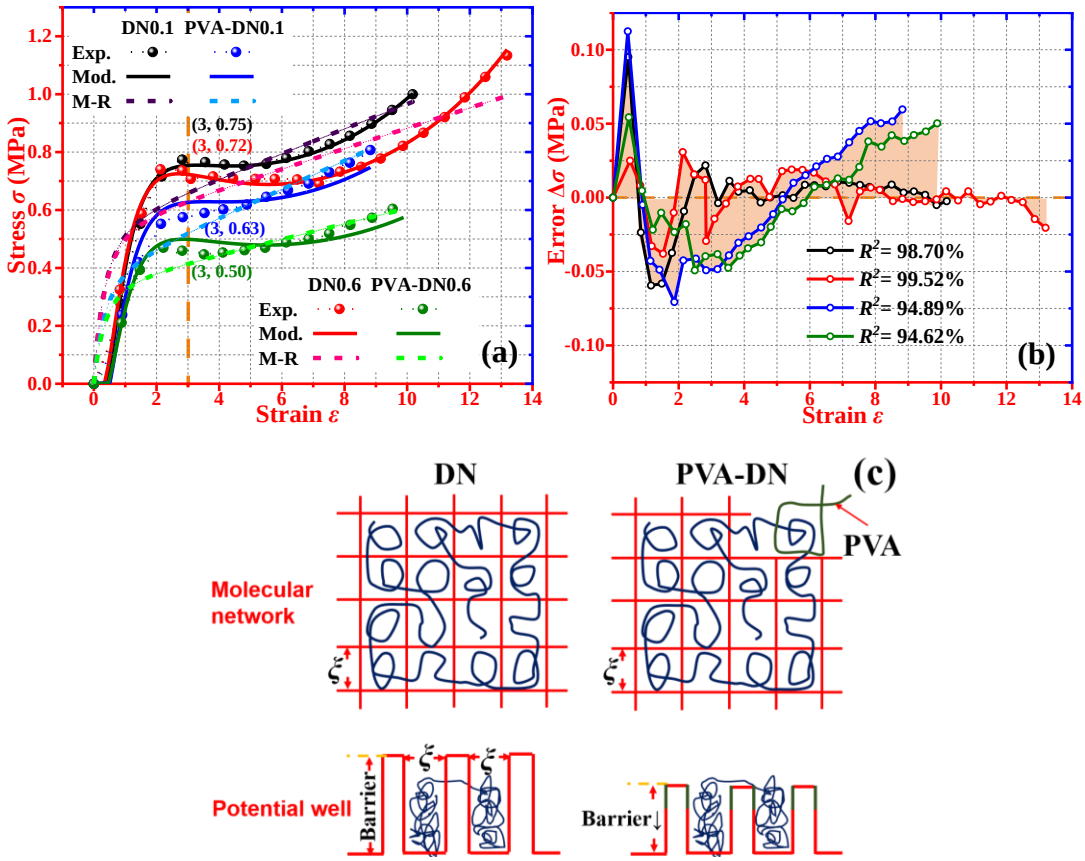

Figure 7. Comparisons among analytical results using equation (15), using the classical Mooney-Rivlin (M-R) model [34], and experimental data [25] of the stress as a function of strain for PAMPS/PAAm DN hydrogels. (a) The stress-strain curves. (b) Divergences of analytical and experimental results of stress. (c) Schematic illustration of the effect of depth (barrier energy, F_{ba}) on the stress-strain behavior in PAMPS/PAAm DN and PVA-DN hydrogels.

The working principle of the PAMPS/PAAm DN and PVA-DN hydrogels is illustrated in Figure 7(c). With an increase in photo-initiator from 0.1 mol% to 0.6 mol%, or introducing PVA, the modulus of PAMPS brittle networks is decreased with

a decrease in depth of potential well in DN hydrogels, resulting from the decrease in the barrier energy (F_{ba}).

Table 3. Values of parameters used in equation (15) for PAMPS/PAAm DN hydrogels.

	$N_{el}k_BTp_0$(MPa)	ξ_0/b	m	$2D_e/k_BT$	ΔR_0(Å)	ρ_{ea}
DN0.1	0.153	20	237	405 [29]	0.008	0.42
PVA-DN0.1	0.128		249			
DN0.6	0.180	11	80			
PVA-DN0.6	0.126		85			

Figure 8(a) plots both the calculated and experimental stress-strain relationships for the PAMPS/PAAm DN hydrogels with different void ratios of brittle PAMPS networks of 0 vol%, 1 vol%, 3 vol% and 10 vol% [24]. All the parameters used in the calculations using the equation (15) are listed in Table 4. With the increase in the void ratios from 0 vol%, 1 vol%, 3 vol% to 10 vol%, the stress was decreased from 0.88 MPa, 0.82 MPa, 0.73 MPa to 0.60 MPa at the same strain of ε=3. Moreover, the correlation index (R^2) between the analytical and experimental results were calculated to be 95.10%, 98.63%, 97.65% and 98.71% for 0 vol%, 1 vol%, 3 vol% and 10 vol% PAMPS/PAAm DN hydrogels, respectively, as shown in Figure 8(b). It can be seen that the analytical results agree well with the experimental data [24], where the divergence of stress is limited to $|\Delta\sigma|$<0.15 MPa.

Effects of depth of brittle network (i.e., the barrier energy, F_{ba}) on the PAMPS/PAAm DN hydrogel have further been analysed, and the obtained results are shown in Figure 8(c). With an increase in void ratio of PAMPS brittle network, the depth (or the barrier energy, F_{ba}) of brittle network is decreased, mainly due to the

decrease in host-guest interaction between two networks of PAMPS and PAAm.

Table 4. Values of parameters used in equation (15) for PAMPS/PAAm DN hydrogels.

vol%	$N_{el}k_BTp_0$(MPa)	ξ_0/b	m	$2D_e/k_BT$	ΔR_0(Å)	ρ_{ea}
0	0.233	9	59	405 [29]	0.008	0.42
1	0.210	10	67			
3	0.182	11	85			
10	0.136	14	127			

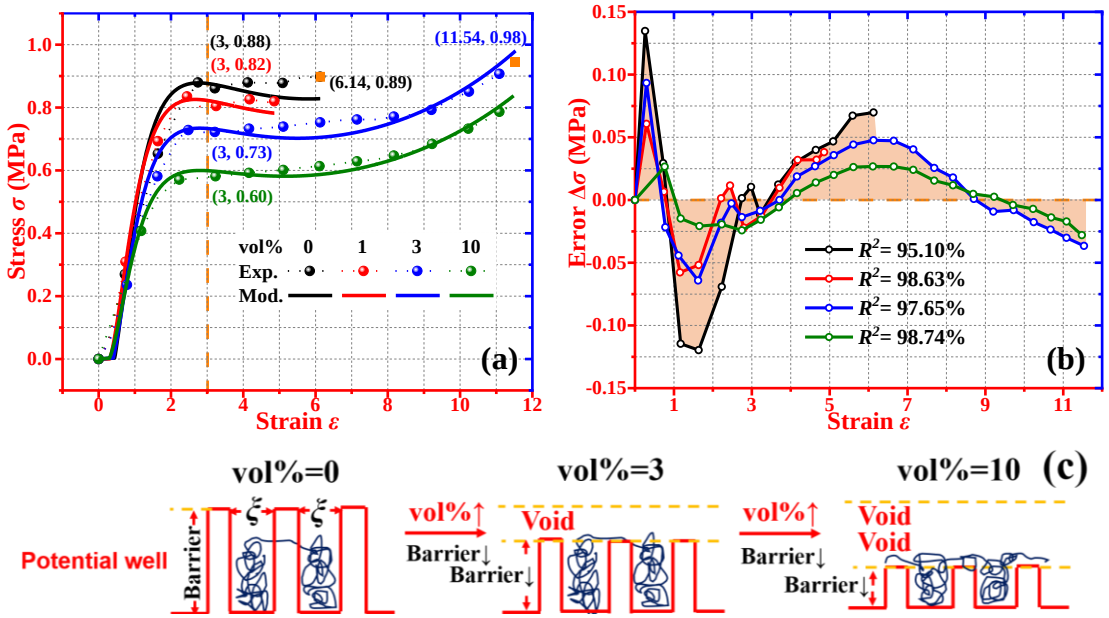

Figure 8. Comparisons of analytical results using equation (15) and experimental data [24] of the stress as a function of strain for PAMPS/PAAm DN hydrogels. (a) The stress-strain curves. (b) Divergences of analytical and experimental results of stress. (c) Schematic illustration of the effect of depth (barrier energy, F_{ba}) on the stress-strain behavior.

4. Conclusions

In this study, a potential well model is established to understand the mechanochemical coupling and toughening mechanism of host-guest chemistry in the DN hydrogels, where the width, depth and trap number of potential wells have been employed to describe the mesh size, barrier energy and mechanochemical interaction, respectively. Analytical and experimental results reveal that the width, depth and trap

number of potential wells play essential roles to determine the elasticity, yielding and mechanochemical behaviors of the DN hydrogels, respectively. Furthermore, the mechanochemical coupling and toughening mechanism have been identified by the parameters of width, depth and trap number of the proposed potential well model. Finally, effectiveness of the proposed model is verified using FEA and experimental results of DN hydrogels reported in literature. Good agreements among analytical, simulation and experimental results have been obtained. This study clarifies the toughening mechanism and identifies the mechanochemical coupling in DN hydrogels, of which the host-guest chemistry has been investigated using the potential well model.

Acknowledgements

This work was financially supported by the National Natural Science Foundation of China (NSFC) under Grant No. 11725208 and 12172107, International Exchange Grant (IEC/NSFC/201078) through Royal Society UK and the NSFC.

References

[1] de Gennes P G 1992 Soft Matter *Reviews of Modern Physics* **64** 645-8

[2] Zhao X H 2017 Designing toughness and strength for soft materials *Proc. Natl. Acad. Sci. USA* **114** 8138-40

[3] Rumyantsev A M, Jackson N E and de Pablo J J 2021 Polyelectrolyte complex coacervates: recent developments and new frontiers *Annu. Rev. Condens. Matter Phys.* **12** 155-76

[4] Long R, Hui C-Y, Gong J P and Bouchbinder E 2021 The fracture of highly deformable soft materials: a tale of two length scales *Annu. Rev. Condens. Matter Phys.* **12** 71-94

[5] Sun J Y, Zhao X, Illeperuma W R K, Chaudhuri O, Oh K H, Mooney D J, Vlassak J J and Suo Z 2012 Highly stretchable and tough hydrogels *Nature* **489** 133-6

[6] Matsuda T, Kawakami R, Namba R, Nakajima T and Gong J P 2019 Mechanoresponsive self-growing hydrogels inspired by muscle training *Science* **363** 504-8

[7] Benitez-Duif P A, Breisch M, Kurka D, Edel K, Gökcay S, Stangier D, Tillmann W, Hijazi M and Tiller J C 2022 Ultrastrong poly(2-oxazoline)/poly(acrylic acid) double-network hydrogels with cartilage-like mechanical properties *Adv. Funct. Mater.* **32** 2204837

[8] Zhang X, Yao D, Zhao W, Zhang R, Yu B, Ma G, Li Y, Hao D and Xu F J 2021 Engineering platelet-rich plasma based dual-network hydrogel as a bioactive

wound dressing with potential clinical translational value. *Adv. Funct. Mater.* **31** 2009258

[9] Huang C, Luo Q, Miao Q, He Z, Fan P, Chen Y, Zhang Q, He X, Li L and Liu X 2022 MXene-based double-network organohydrogel with excellent stretchability, high toughness, anti-drying and wide sensing linearity for strain sensor *Polymer* **253** 124993

[10] Li G, Huang K, Deng J, Guo M, Cai M, Zhang Y and Guo C F 2022 Highly conducting and stretchable double-network hydrogel for soft bioelectronics *Adv. Mater.* **34** 2200261

[11] Xu X, Jerca V V and Hoogenboom R 2021 Bioinspired double network hydrogels: from covalent double network hydrogels via hybrid double network hydrogels to physical double network hydrogels *Mater. Horiz.* **8** 1173

[12] Chen Q, Chen H, Zhu L and Zheng J 2015 Fundamentals of double network hydrogels *J. Mater. Chem. B* **3** 3654-76

[13] Webber R E, Creton C, Brown H R and Gong J P 2007 Large strain hysteresis and Mullins effect of tough double-network hydrogels *Macromolecules* **40** 2919-27

[14] Jang S S, Goddard W A and Kalani M Y S 2007 Mechanical and transport properties of the poly (ethylene oxide)-poly (acrylic acid) double network hydrogel from molecular dynamic simulations *J. Phys. Chem. B* **111** 1729-37

[15] Gong J P, Katsuyama Y, Kurokawa T and Osada Y 2003 Double-network hydrogels with extremely high mechanical strength *Adv. Mater.* **15** 1155-8

[16] Gong J P 2010 Why are double network hydrogels so tough? *Soft Matter* **6** 2583-90

[17] Yue Y F, Li X F, Kurokawa T and Gong J P 2016 Decoupling dual-stimuli responses in patterned lamellar hydrogels as photonic sensors *J. Mater. Chem. B.* **4** 4104-09

[18] Xiang Y H, Zhong D M, Wang P, Yin T H, Zhou H F, Yu H H, Baliga C, Qu S X and Yang W 2019 A physically based visco-hyperelastic constitutive model for soft materials *J. Mech. Phys. Solids* **128** 208-18

[19] Xiang Y H, Zhong D M, Wang P, Mao G Y, Yu H H and Qu S X 2018 A general constitutive model of soft elastomers *J. Mech. Phys. Solids* **117** 110-22

[20] Lau D, Broderick K, Buehler M J and Buyukozturk O 2014 A robust nano-scale experimental quantification of fracture energy in a bi-layer material system *P Natl. Acad. Sci. USA* **111** 11990-11995

[21] Zhang H J, Sun TL, Zhang A K, Nakajima T, Nonoyama T, Kurokawa T, Ito O, Ishitobi H and Gong J P 2016 Tough physical double-network hydrogels based on amphiphilic triblock copolymers *Adv. Mater.* **28** 4884-90

[22] Wang Z, Zheng X, Ouchi T, Kouznetsova T B, Beech H K, Av-Ron S, Matsuda T, Bowser B H, Wang S, Johnson J A, Kalow J A, Olsen B D, Gong J P, Rubinstein M and Craig S L 2021 Toughening hydrogels through force-triggered chemical reactions that lengthen polymer strands *Science* **374** 193-6

[23] Yin H, King D R, Sun T L, Saruwatari Y, Nakajima T, Kurokawa T and Gong J P 2020 Polyzwitterions as a versatile building block of tough hydrogels: from

polyelectrolyte complex gels to double-network gels *ACS Appl. Mater. Inter.* **12** 50068-76

[24] Nakajima T, Furukawa H, Tanaka Y, Kurokawa T and Gong J P 2011 Effect of void structure on the toughness of double network hydrogels *J. Polym. Sci. Part B Polym. Phys.* **49** 1246-54

[25] Nakajima T, Takedomi N, Kurokawa T, Furukawa H and Gong J P 2010 A facile method for synthesizing free-shaped and tough double network hydrogels using physically crosslinked poly(vinyl alcohol) as an internal mold *Polym. Chem.* **1** 693-7

[26] Ducrot E, Chen Y, Bulters M, Sijbesma R P and Creton C 2014 Toughening elastomers with sacrificial bonds and watching them break *Science* **344** 186-9

[27] Li X, Cui K, Kurokawa T, Ye Y N, Sun T L, Yu C, Creton C and Gong J P 2021 Effect of mesoscale phase contrast on fatigue-delaying behavior of self-healing hydrogels *Sci. Adv.* 7 eabe8210

[28] Zheng Y, Kiyama R, Matsuda T, Cui K, Li X, Cui W, Guo Y, Nakajima T, Kurokawa T and Gong J P 2021 Nanophase separation in immiscible double network elastomers induces synergetic strengthening, toughening, and fatigue resistance *Chem. Mater.* **33** 3321-34

[29] Charan H, Hansen A, Hentschel H G E and Procaccia I 2021 Aging and failure of a polymer chain under tension *Phys. Rev. Lett.* **126** 085501

[30] Lau D, Buyukozturk O, Buehler M J 2012 Characterization of the intrinsic strength between epoxy and silica using a multiscale approach *J. Mater. Res.* **27** 1787-1796

[31] Rouse P E 1953 A Theory of the linear viscoelastic properties of dilute solutions of coiling polymers *J. Chem. Phys.* **21** 1272-80

[32] Jia D and Muthukumar M 2021 Electrostatically driven topological freezing of polymer diffusion at intermediate confinements *Phys. Rev. Lett.* **126** 057802

[33] Flory P J 1953 Principles of Polymer Chemistry New York: Cornell University Press

[34] Treloar L R G 1975 The Physics of Rubber Elasticity New York: Oxford University

[35] de Gennes P G 1979 Scaling Concepts in Polymer Physics. Ithaca and London: Cornell University Press

[36] Kosovan P, Richter T and Holm C 2015 Modeling of polyelectrolyte gels in equilibrium with salt solutions *Macromolecules* **48** 7698-708

[37] Hua J, Mitra M K and Muthukumar M 2012 Theory of volume transition in polyelectrolyte gels with charge regularization *J. Chem. Phys.* **136** 134901

[38] Mohanta D, Giri D and Kumar S 2022 Effect of solvent gradient inside the entropic trap on polymer migration *Phys. Rev. E* **105** 024135

[39] Jung Y, Jun S and Ha B-Y 2009 Self-avoiding polymer trapped inside a cylindrical pore: Flory free energy and unexpected dynamics *Phys. Rev. E* **79** 061912